TIR-BASED DYNAMIC LIQUID-LEVEL AND FLOW-RATE SENSING AND ITS APPLICATION ON CENTRIFUGAL MICROFLUIDIC PLATFORMS

J. Hoffmann[1,‡], L. Riegger[2,‡], D. Mark[1], F. von Stetten[1], R. Zengerle[1,2], J. Ducrée[3]
[1] HSG-IMIT, Villingen-Schwenningen, GERMANY
[2] IMTEK - University of Freiburg, Freiburg, GERMANY
[3]BDI, Dublin City University, Dublin, IRELAND
[‡] contributed equally

ABSTRACT

For the first time we present a technique for the spatio-temporally resolved localization of liquid-gas interfaces on centrifugal microfluidic platforms based on total internal reflection (TIR) at the channel wall. The simple setup consists of a line laser and a linear image sensor array mounted in a stationary instrument. Apart from identifying the presence of (usually unwanted) gas bubbles, the here described online meniscus detection allows to measure liquid volumes with a high precision of 1.9 %. Additionally, flow rates and viscosities (range: 1 – 10.7 mPa s) can be sensed even during rotation at frequencies up to 30 Hz with a precision of 4.7 % and 4.3 %, respectively.

INTRODUCTION

Microfluidic lab-on-a-chip systems make use of the rescaling of hydrodynamic force ratios in miniaturized fluidic networks. Towards the micron world, surface-to-volume ratios significantly increase, thus making surface mediated effects such as surface tension and viscous drag prevail over bulk forces such as inertia and gravity.

Lab-on-a-chip devices typically concatenate laboratory unit operations for liquid handling such as sample preparation, aliquoting, metering, and mixing on a single substrate [1,2] to perform bio-chemical assays in a process-integrated, automated, miniaturized and often parallel fashion. However, due to their strong dependency on often hard to control surface properties, lab-on-a-chip systems are intrinsically prone to inconsistencies such as the formation of gas bubbles or pockets during priming and operation. This tendency may lead to insufficient filling of microfluidic cavities with sample or reagents. In order to leverage a successful transfer of academic lab-on-a-chip technology to real-world applications, it is therefore key to introduce a quality control which monitors the course of liquid filling.

To this end, we recently presented a technique based on TIR on the channel wall to localize liquid-gas interfaces in microchannels at rest [3]. In this contribution, we present for the first time its implementation on a centrifugal microfluidic platform [4]. Our technique is based on linear illumination and detection elements allowing quasi-continuous meniscus detection with a spatial resolution of 50 µm at high speeds of rotation up to 30 Hz.

SETUP

The experimental setup consists of a rotatable lab-on-a-chip substrate (also referred to as lab-on-a-disk), and a device (called the "player") which accommodates the optical components and spins at well defined rotational frequencies and acceleration rates.

Disk Design and Fabrication

The disk contains four pairs of channels aligned at 90°-offset to each other according to the symmetry of the disk as illustrated in Figure 1.

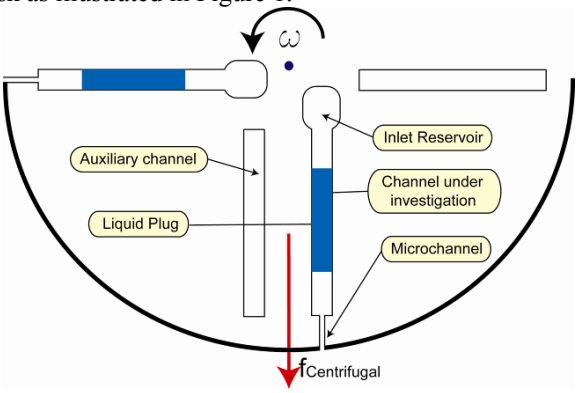

Figure 1: Schematic of the on-disk structure, showing all relevant channels and geometric features referred to in this section.

Each channels pair is laterally shifted with respect to a central radial line. The channel under investigation and the auxiliary channel possess a triangular cross-section, each possessing a wall inclination angle of 45° ("V-groove"). These channels are illuminated by a laser from the top, i.e. from a direction perpendicular to the plane of the disk. According to Snell's law TIR occurs for a perpendicular incidence in case the ratio of refractive indices of the bulk material of the disc and the medium inside the channel exceeds 1.41 at the location of the inclined channel wall. This condition is fulfilled for a gas filled channel segment, but not in the presence of a liquid.

Said channels have a depth of 1.5 mm and a width of 3 mm. The four inner endings of the channels near the center of rotation are flanked by an inlet reservoir. The radially outer side of the channel leads to a rectangular channel measuring 400 µm in width, 100 µm in depth, and ~ 4 mm in length, referred to as the "microchannel". The other four V-grooves are auxiliary channels which are permanently filled with air.

The 2-D fluidic design of the disk is generated by a CAD software. It provides the code for a micromilling machine which creates the corresponding 2.5-D design

within a cyclo olefin colpolymer (COC) substrate (refractive index n = 1.49). The total time from design to the fabricated disk takes approximately 4 hours (depending on the complexity of the fluidic design).

Optical and Read-out Components

The optical measurement components are a line laser and a linear image sensor array. The laser diode emits at the peak-wavelength λ_{peak} = 650 nm having a maximum optical power of 24 mW (Roithner RLLH 650-24-3). The housing contains this diode as well as a special line optics generating the probe line. The used CMOS linear image sensor (Hamamatsu S8377) is a compact sensor featuring a built-in timing generator as well as signal processing circuit. The active area has a length of 25.6 mm subdivided into 512 individual pixels (pixel pitch: 50 µm, pixel height: 500 µm).

An electrical controlling unit (Spectronics Devices) is used to address the operating mode of the sensor as well as to transfer optical data to a PC. The set comprises two small size printed circuit boards (PCB): a small 50 mm x 20 mm PCB holding the sensor incorporating a pre-amplifier and A/D converter electronics and a second PCB with the control electronics, a 1-MByte data storage memory for saving 1000 scans and a USB PC-interface. The processing time for one scan takes 2 µs, only, which allows the here required high-speed data acquisition.

OPERATING PRINCIPLE

Figure 1-A illustrates the functional principle for the TIR-based meniscus detection while the experimental setup is depicted in Figure 1-B:

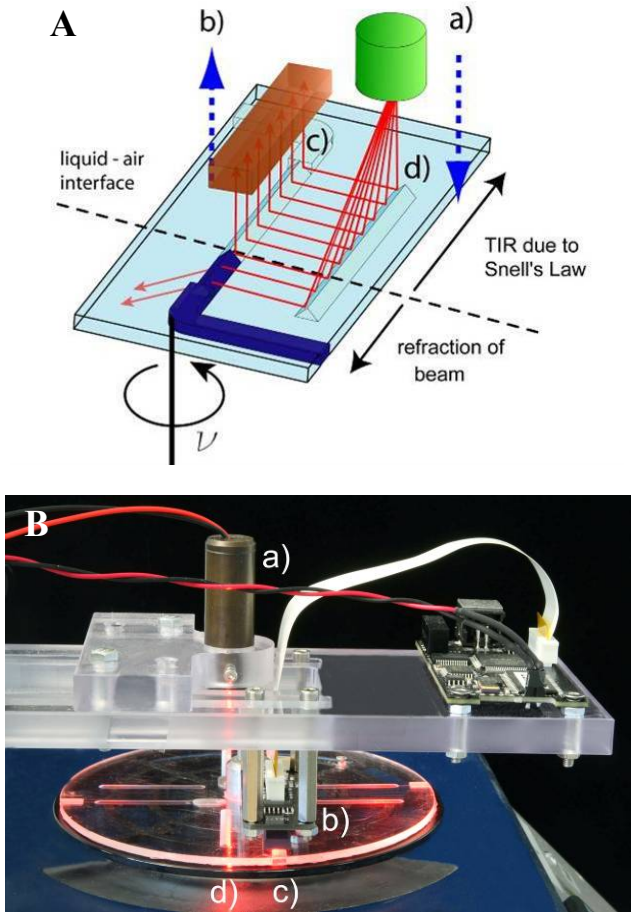

Figure 2: (A) Setup of TIR-based meniscus detection. (B) Photo of the experimental setup. The beam is issued from a line laser onto the rotating substrate and reflected back to a linear image sensor. Legend: a) line laser b) linear image sensor c) channel under investigation d) auxiliary channel.

Optical Pathway

The beam emitted by the line laser (a) impinges on an auxiliary, permanently air-filled channel (d). Due to the 45° inclination of its respective wall, the beam is deflected by 90° into the plane of the substrate. After a defined distance corresponding to the spacing between the laser and the detector, the beam impinges on the V-grooved segment of the channel under investigation (c). If a probed segment is filled with air, a second TIR redirects the laser beam by 90° towards the linear image sensor (b) placed perpendicular to the plane of the disk. The segments of the channel which are filled by liquid change the local refractive index and rule out TIR.

The emitting power of the line laser is set to a value (5 mW), thus always driving those pixels of the sensor receiving high intensity into saturation. This way a discrete, binary signal is obtained where 1 indicates an empty section, 0 a liquid-filled section of the channel (c). This works up to frequencies of 30 Hz. At higher frequencies, the received intensity is too low to push the sensor into saturation.

Measurements under Rotation

The azimuthal position of the channels on the disk and the sensor position are synchronized by using the TTL-signal provided by the player once per revolution as a command-signal for the sensor. The linear image sensor starts to acquire optical data each time the rising flank of the trigger signal occurs and stops after a certain integration time derived from the frequency of rotation. The integration time is set to a value that each revolution a disk-sector spanning over channels (c) and (d) is covered. Thereby, a consistent and stable measurement system is guaranteed requiring no alignment or signal strength calibration.

EXPERIMENTS

Bubble Detection

A representative plot for the pixel intensity along a channel entrapping an air bubble under static conditions is shown in Figure 2, revealing clearly discernible edges at the respective liquid-gas interfaces. Using proper curve fitting algorithms, the position of the meniscus can be pinpointed down to roughly 3 pixels, corresponding to 150 µm.

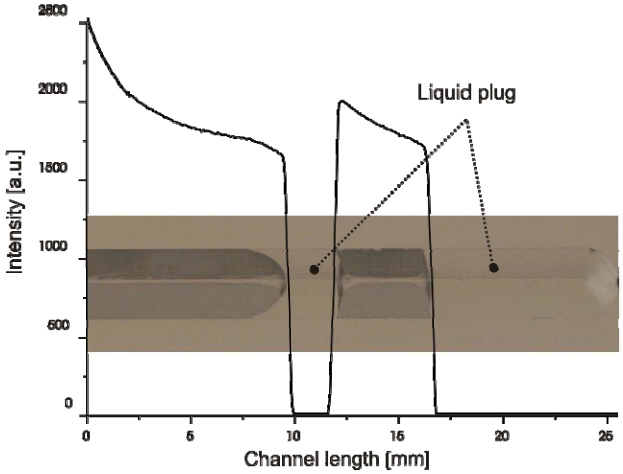

Figure 3: Measured pixel intensity plot of a bubble within a channel captured by the linear image sensor at rest. The transition between the liquid and the gas state is very distinct thus allowing a clear localization of the meniscus.

Volume Calibration

The detection of gas bubbles and liquid filling levels are essential to assure reproducible and quantitative bioassays on LoaC systems. This section describes the calibration of our TIR-based measurement system to meet these requirements. Figure 3 displays a calibration curve with five pre-metered volumes, featuring a high accuracy and a precision of 1.9 %.

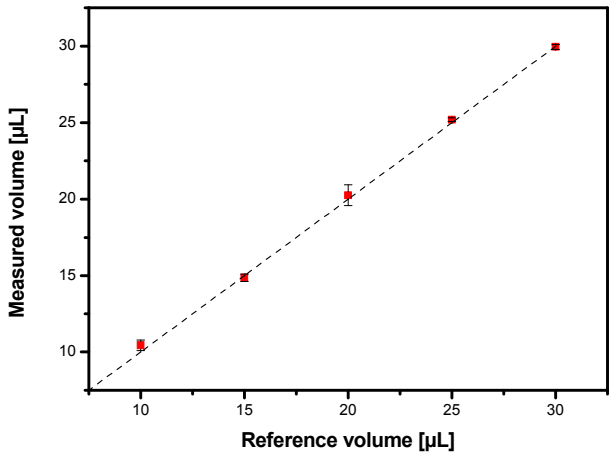

Figure 4: Calibration of the measured volumes with pre-metered volumes featuring a high precision of 1.9 %.

For a fixed microchannel geometry, the theoretical maximum filling level is calculated with respect to the length of the channel. In the next step, the active area of the linear image sensor is laterally shifted (positioned) in such a way that it provides output characteristics corresponding to the calculated liquid level. Once the system is calibrated, the measurements described in the following sections are performed. For the volume calibration, liquid-levels of five different volumes (10, 15, 20, 25 and 30 µL) are measured five times each. Each measurement is conducted under rotation at 10 Hz whereby the position of the liquid-gas interface is averaged over 10 revolutions with one measurement per revolution. Figure 3 shows the capability of this system to accurately measure and meter liquid volumes during rotation.

Flow Rates and Viscosities

Centrifugally driven discharge induced by a constant rotational frequency of 10 Hz is presented in Fig. 4. Tests are based on four different glycerol solutions with dynamic viscosities in the range of 1 – 10.7 mPa s.

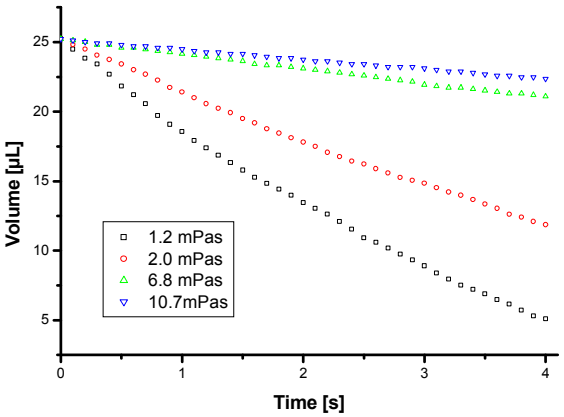

Figure 5: Flow rate and viscosity measurements derived from a time-resolved liquid-level determination with the calibrated system. The relative decrease of the flow rate correlates with increasing viscosity.

25 µL of each sample liquid are pipetted into the inlet reservoir. Fluids are driven through the inclined channel by centrifugal forces and introduced into the adjoining microchannel. The flow rate in the microchannel itself is indirectly measured via the movement of the liquid-gas interface in the channel under investigation using a curve-fitting algorithm.

Four different liquids with viscosities of 1.2, 2, 6.8, and 10.7 mPa s are investigated. The time resolved measurements for each moving liquid reveal the $1/\eta$ dependence for the flow rate during the outflow. Also, with the dynamically decreasing plug position, a multi-parameter dependent flow rate can be identified. The motion of the meniscus is affected by the spinning frequency, interfacial interactions, microchannel geometries, and the viscosity of the fluid.

Contact-free and on-line determination of the flow rate provides an insight into liquid guidance on lab-on-a-disk systems. Furthermore, the implementation of a feedback-loop can improve the liquid guidance on-disk and contribute to a better controllable fluidic system.

Figure 5 demonstrates the capability of the system to measure the dynamic viscosity of low-viscosity liquids. The unprecedented dynamic recordings of the flow rates and viscosities during rotation are enabled by the linear optical elements in contrast to the static scanning principle of our previous work [3].

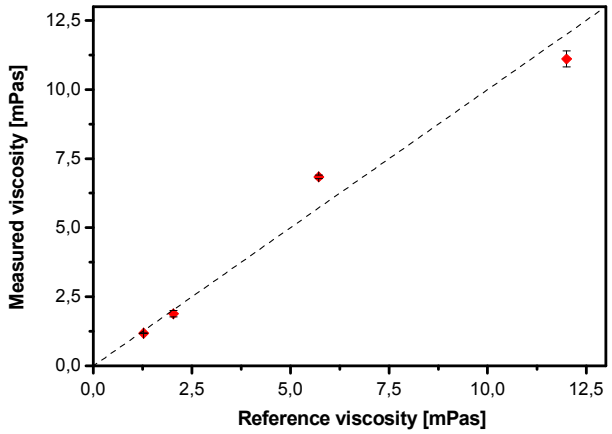

Figure 6: Dynamic viscosity measurement featuring a precision of 4.3 % for viscosities up to 10.7 mPa s.

The previously described glycerol solutions are used to highlight the correlation between the measured viscosities and the reference viscosities. First, defined volumes (25 µL) are introduced into the channel under investigation and centrifugally pumped at a constant frequency of ν = 10 Hz through the connected microchannel. Each flow rate is measured five times.

Secondly, the viscosity is calculated taking the following physical parameters into account: flow rate and position of the passing liquid plug, temperature, angular frequency and the dimensions of the microchannel. A precision of 4.3 % is a good result compared to rheology measuring devices struggling with difficulties in the low viscosity regime. In addition to flow rates of unknown samples, our system reveals absolute viscosity data as a surplus.

CONCLUSION

This work investigates a novel TIR-based setup with linear optical elements for spatio-temporally resolved meniscus detection. The system is well suited for compact system integration and excels with its high-speed data acquisition and low cost compared to conventional image processing systems.

Due to the simple integration of the auxiliary channel structures in the microfabrication process of the substrate as well as the uncomplicated component upgrade of the disk-processing unit, the opto-fluidic technology can be easily incorporated into centrifugal microfluidic systems.

The system can be used for quality control, feedback loop and calibration purposes on centrifugal lab-on-a-disk platforms, e.g. for the on-line verification or liquid filling or outflow, for monitoring the flow of a liquid plug, for reagent metering or viscosity measurements of unknown patient samples. The contactless measuring principle does not require any pretreatment of the fluid, e.g. the introduction of particles, and prevents any impact on the fluidic function itself.

Implementation of our measurement system into real-world point-of-care devices could significantly improve the quality of assay results by the real-time monitoring of liquid levels, flow rates, viscosities and gas bubble formation in liquid handling operations.

REFERENCES

[1] P. S. Dittrich and A. Manz, "Lab-on-a-chip: microfluidics in drug discovery," *Nature Reviews Drug Discovery*, vol. 5, no. 3, pp. 210-218, Mar.2006.

[2] J. Y. Park and L. J. Kricka, "Prospects for nano- and microtechnologies in clinical point-of-care testing," *Lab Chip*, vol. 7, no. 5, pp. 547-549, 2007.

[3] F. Bundgaard, O. Geschke, R. Zengerle, and J. Ducrée, "A simple opto-fluidic switch detecting liquid filling in polymer-based microfluidic systems," in *Proceedings of the 14th International Conference on Solid-State Sensors, Actuators and Microsystems (Transducers & Eurosensors '07)* Lyon, France: 2007, pp. 759-762.

[4] J. Ducrée, S. Haeberle, S. Lutz, S. Pausch, F. von Stetten, and R. Zengerle, "The centrifugal microfluidic Bio-Disk platform," *J. Micromech. Microeng.*, vol. 17, p. S103-S115, 2007.